DOI: 10.1002/ejic.201100804

A Highly Selective Fluorescent and Colorimetric Chemosensor for Zn^{II} and Its Application in Cell Imaging

Guoqiang Xie,[a] Yanjun Shi,[a] Fengping Hou,[a] Hongyan Liu,[a] Liang Huang,[a] Pinxian Xi,[a] Fengjuan Chen,[a] and Zhengzhi Zeng*[a]

Keywords: Fluorescence / Zinc / N ligands / Colorimetric chemosensor / 8-Aminoquinoline / Cell imaging

A fluorescent, colorimetric chemosensor, **L1**, based on 8-aminoquinoline, has been developed as a sensor for Zn^{2+}. **L1** exhibited high selectivity and sensitivity towards Zn^{2+} over other common metal ions in a physiological pH window with a 1:1 binding mode. The ability of **L1** to monitor intracellular Zn^{2+} in living cells has been examined by fluorescence microscopy and indicated that **L1** is cell-permeable and biocompatible. We hope that such Zn^{2+}-selective sensors will find application in biomedical and environmental detection.

Introduction

The development of fluorescent chemosensors that have the capability to selectively recognize and sense metal ions is one of the most challenging fields in organic and supramolecular chemistry.[1] Sensors based on ion-induced changes (e.g. intensity and/or emission wavelength) in fluorescence have many advantages over other techniques, which include their simplicity, high sensitivity, high selectivity, and instantaneous response.[2] So far, a number of excellent metal-ion sensors based on metal–ligand coordination or chemical reaction have been reported to detect transition and heavy metal ions, such as zinc ions.[3] Zinc is the second most abundant transition metal in human body after iron and plays important roles in various pathological processes.[4] Zn^{2+} does not give any spectroscopic or magnetic signals due to its $3d^{10}4s^0$ electronic configuration. However, fluorescence is an effective way to detect zinc in biological systems.

Considerable efforts have been made to design and synthesize fluorescent chemosensors for Zn^{2+}.[5] Among the various fluorescent sensors, 8-aminoquinoline and its derivatives are the first class of probes to have been developed for Zn^{2+}.[6] They exhibit good photostability, high affinity to metal ions, and satisfactory membrane permeability.[7] Despite some commercial fluorescent probes for Zn^{2+},[8] the design of facile, easy to synthesize, nontoxic Zn^{2+}-selective sensors is still a challenging task, and there is a need for the design and synthesis of such chemosensors, which are small molecules and highly sensitive for real-time detection in biological systems at physiological pH.

We have synthesized a new 8-aminoquinoline derivative **L1** as a Zn^{2+} chemosensor, which shows high sensitivity and selectivity for Zn^{2+} over other possible competitive cations based on internal charge transfer (ICT) and chelation-enhanced fluorescence mechanisms. The mode of binding of **L1** with Zn^{2+} was investigated by UV/Vis spectrophotometric titration and fluorescence titration. The ability of **L1** to detect Zn^{2+} in living cells was examined by fluorescence microscopy.

Results and Discussion

L1 was easily prepared from 8-aminoquinoline and rhodamine 6G in high yield (Scheme 1), and its structure was confirmed by ^1H and ^{13}C NMR spectroscopy, ESI-MS (see Supporting Information), and X-ray diffraction (Figure 1).

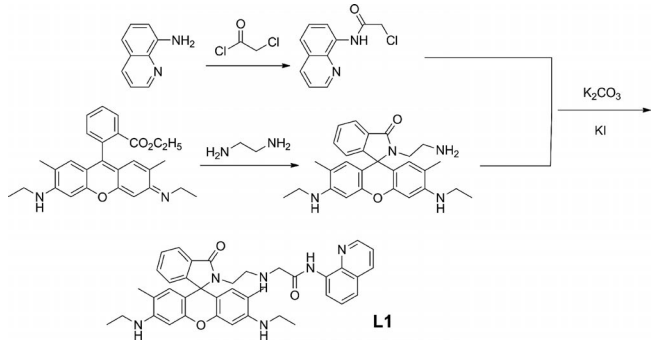

Scheme 1. Synthetic route to **L1**.

[a] Key Laboratory of Nonferrous Metal Chemistry and Resources Utilization of Gansu Province,
Lanzhou 730000, P. R. China
Fax: +86-931-8912582
E-mail: zengzhzh@yahoo.com.cn
zengzhzh@lzu.edu.cn

Supporting information for this article is available on the WWW under http://dx.doi.org/10.1002/ejic.201100804.

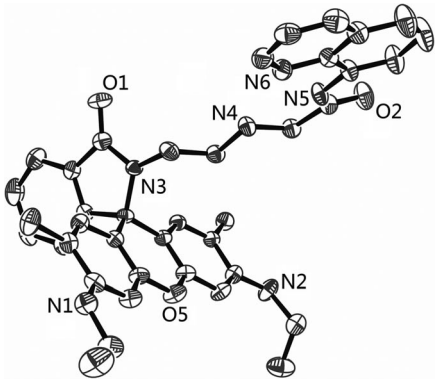

Figure 1. X-ray crystal structure of **L1**. All hydrogen atoms are omitted for clarity (50% probability level for the thermal ellipsoids).

The mode of coordination of **L1** with Zn^{2+} was investigated by spectrophotometric titration in acetonitrile solution. Figure 2a shows the spectral variation of **L1** with the gradual addition of Zn^{2+}. The absorbance of **L1** at 237 and 303 nm decreased linearly with increasing concentration of Zn^{2+}. In addition, two new absorption peaks appeared at 256 and 362 nm, and their intensity increased with the addition of Zn^{2+}, which was accompanied by three isosbestic points at 247, 282, and 340 nm, respectively. These phenomena are expected to correspond to the coordination of **L1** with Zn^{2+}, which extended the conjugated system and resulted in the appearance of the new absorption in the long-wavelength region.[9] According to the linear Benesi–Hildebrand expression,[10] the measured absorbance $[1/(A - A_0)]$ at 362 nm varied as a function of $1/[Zn^{2+}]$ in a linear relationship (R^2 = 0.9980), which indicates a 1:1 stoichiometry between Zn^{2+} and **L1** (Figure 2b). Moreover, there were no absorption peaks between 450 and 700 nm, which indicates that the spirolactam rhodamine was not ring-opened and the N3 atom does not participate in the coordination to Zn^{2+}.

The spectrum of **L1** (10 μM) showed a weak emission at around 499 nm (λ_{ex} = 365 nm, fluorescence intensity, F_0 = 14.4, quantum yield, Φ_0 = 0.005) in acetonitrile solution. As shown in Figure 3, the addition of Zn^{2+} (0–15 μM) to the solution produced a new emission band centered at 499 nm with an approximately 77-fold enhancement in intensity (Φ = 0.537).

The fluorescence titration profile of **L1** with Zn^{2+} demonstrates that the detection of Zn^{2+} is 1 μM in the range of 0–15 μM of $[Zn^{2+}]$. These results can be explained as follows. After binding with Zn^{2+}, the intramolecular electron-transfer process becomes forbidden, which enhances the fluorescence emission.[11] Simultaneously, the electron transfer from the nitrogen atom of the heterocycle to the metal ion enhances the ICT process.[12] Another reason for enhanced fluorescence could be that a more rigid structure forms when Zn^{2+} binds with **L1**. The association constant for Zn^{2+} was estimated to be 2.9×10^4 M^{-1} on the basis of the linear fit of the titration curve that assumes a 1:1 stoichiometry (Figure S1, Supporting Information). The Job plot (Figure 3, inset) also confirmed that the binding mode had a 1:1 stoichiometry.

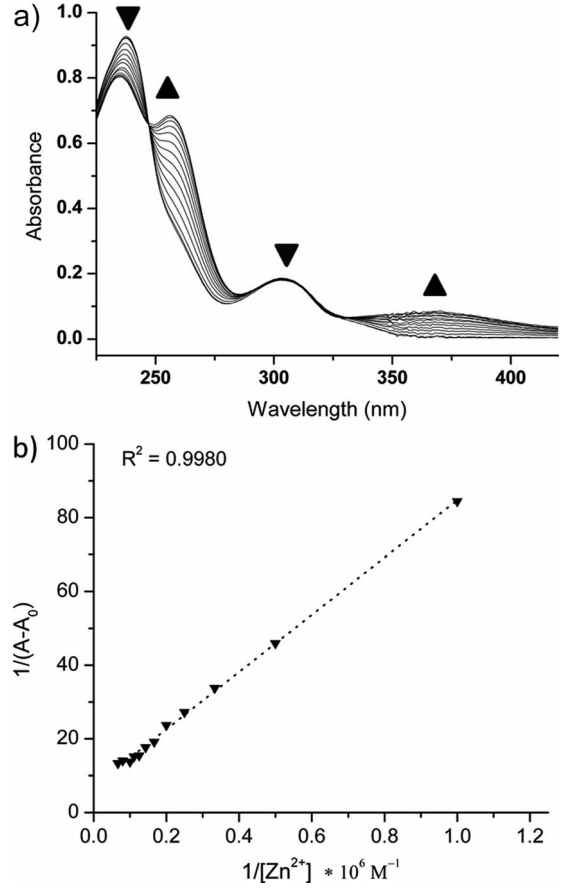

Figure 2. (a) Absorption spectra of **L1** (10 μM) in the presence of Zn^{2+} (0–1 equiv.) in CH_3CN. (b) Plot of $1/(A - A_0)$ at 362 nm as a function of $1/[Zn^{2+}]$.

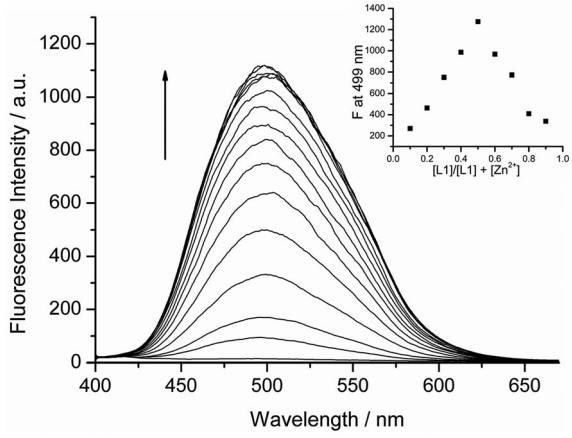

Figure 3. Fluorescence spectra of **L1** (10 μM) in acetonitrile in the presence of different concentrations of Zn^{2+} (0–2 equiv.) excited at 365 nm. Inset: Job plot to determine the stoichiometry of **L1** and Zn^{2+} in acetonitrile (the total concentration of **L1** and Zn^{2+} is 25 μM).

When Zn^{2+} was added to the solution of **L1**, the colorless solution turned pink, and greenish fluorescence was observed by the naked eye. However, the fluorescence did not derive from the fluorophore of rhodamine 6G, because no emission peaks were observed between 530 and 650 nm when we excited the system between 480 and 520 nm. We presumed that the fluorescence of the system originated in the fluorophore of 8-aminoqunoline when excited at 365 nm. Therefore, we can deduce a possible sensing mechanism (Figure 4) in which the spirolactam rhodamine is not ring-opened and three N atoms (labeled N4, N5, and N6 in Figure 1) participate in the coordination to Zn^{2+}.[13] The species that forms in solution has a nearly planar structure. The fourth ligand (X) is NO_3^- by consideration of the charge balance in solution.

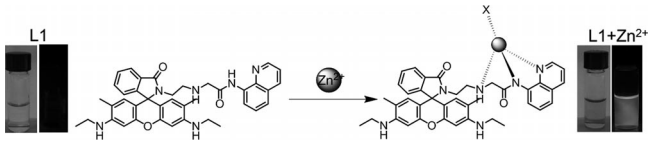

Figure 4. Proposed binding mode of **L1** with Zn^{2+}.

An important property of chemosensors is their high selectivity towards the analyte over the other competitive metal ions. Therefore, we determined the fluorescence intensity of **L1** at 499 nm in the presence of various metal ions. As shown in Figure 5, the addition of Zn^{2+} gave rise to a prominent fluorescence enhancement in an acetonitrile solution of **L1**, whereas the addition of other metal ions, such as K^+, Na^+, Ca^{2+}, and Mg^{2+}, which exist at high concentrations in human cells, did not show any significant color or spectral changes. Fluorescence enhancement of **L1** was observed in the presence of Cd^{2+} because the chemical properties of Cd^{2+} are similar to those of Zn^{2+}. However, the fluorescence intensity of **L1** in the presence of Cd^{2+} is far below that in the presence of Zn^{2+} (F_{Zn}/F_{Cd} = 2.8) under

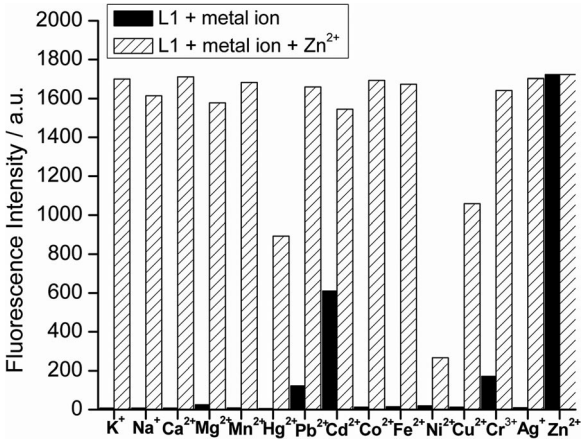

Figure 5. Fluorescence intensities of **L1** (10 μM) in the presence of various metal ions and ion mixtures in acetonitrile. [K^+], [Na^+], [Ca^{2+}], and [Mg^{2+}] = 5 mM, [Zn^{2+}], [Mn^{2+}], [Cr^{3+}], [Pb^{2+}], [Cd^{2+}], [Co^{2+}], [Fe^{2+}], [Ni^{2+}], [Ag^+], [Hg^{2+}], [Cu^{2+}] = 20 μM (λ_{ex} = 365 nm, λ_{em} = 499 nm).

the same conditions, which reflects the lower affinity of **L1** for Cd^{2+}. The fluorescence of the **L1**/Zn^{2+} system was quenched by Ni^{2+}, Cu^{2+}, and Hg^{2+}, which may be due to nonradiative energy transitions or energy transfer between the d orbital of the ions and the fluorophore.[14] These results demonstrate the high selectivity of **L1** towards Zn^{2+}.

For practical applications, the sensing ability of **L1** towards Zn^{2+} at different pH values was investigated (Figure 6). **L1** showed no appreciable fluorescent response to Zn^{2+} in acidic environments due to the more difficult protonation of the imino group (N5) of **L1**, which led to a weak coordination of Zn^{2+}.[15] However, **L1** exhibited satisfactory sensing abilities when the pH was increased from 5.5 to 9.0. These data indicate that **L1** could act as a fluorescent probe for Zn^{2+} under physiological pH conditions.

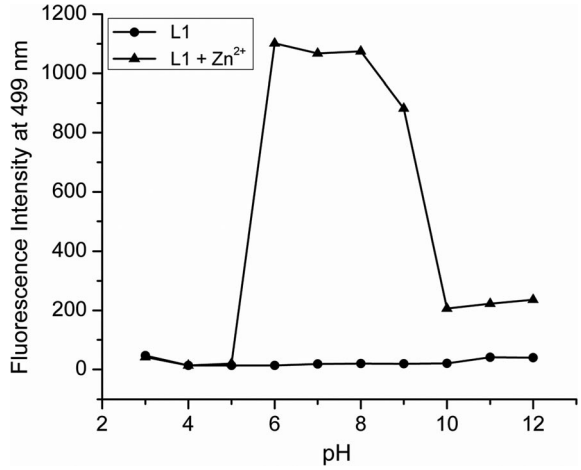

Figure 6. Fluorescence intensities of **L1** (10 μM) in the absence and presence of Zn^{2+} (20 μM) at various pH values in CH_3CN/H_2O (95:5, v/v). (λ_{ex} = 365 nm).

We also investigated the time evolution of the response of **L1** to 2 equiv. of Zn^{2+} in CH_3CN (Figure 7). We found that the interaction of **L1** with Zn^{2+} was completed in less than 2 min. Therefore, this system could be used to track Zn^{2+} in cells and organisms in real-time.

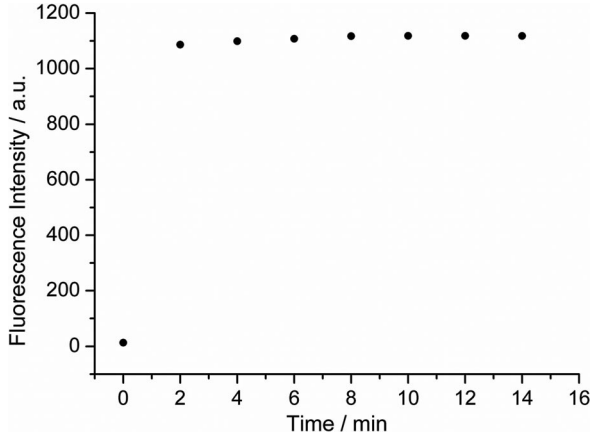

Figure 7. Time evolution of the response of **L1** (10 μM) to 2 equiv. of Zn^{2+} in CH_3CN.

As we developed **L1** to be used with cells, we quantified its effects on the viability of L929 fibroblast cells in vitro. Cell viability was evaluated by using a modified 3-(4,5-dimethylthiazol-2-yl)-2,5-diphenyltetrazolium bromide (MTT) assay. Figure 8 shows the viability of cells treated with **L1** over a range of concentrations for 24, 48, and 72 h. **L1** does not negatively affect cell viability over the full range of concentrations measured, which indicates that they exhibit no cytotoxicity and could be used for intracellular detection.

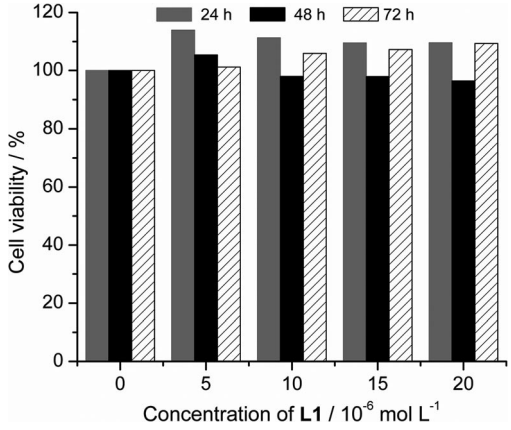

Figure 8. MTT assay of L929 cells cultured for 24, 48, and 72 h in media that contain different amounts of **L1**.

Bright field microscopy images of cells grown in the presence and absence of **L1** confirmed the biocompatibility of **L1** (Figure S2).

The ability of **L1** to detect Zn^{2+} in SCABER (human bladder cancer) cells was also examined. The cells were supplemented with **L1** (10 μM) in Dulbecco's modified Eagle's medium (DMEM) supplemented with 10% fetal bovine serum (FBS) at 37 °C for 3 h and showed very weak intracellular fluorescence as determined by fluorescence microscopy (Figure 9b). With the addition of Zn^{2+} (40 μM) to the treated cells in a culture medium at 37 °C for 0.5 h, a significant increase in fluorescence from the intracellular area was observed (Figure 9d). These results demonstrate that **L1** could be used as a sensor to detect intracellular Zn^{2+} in living cells.

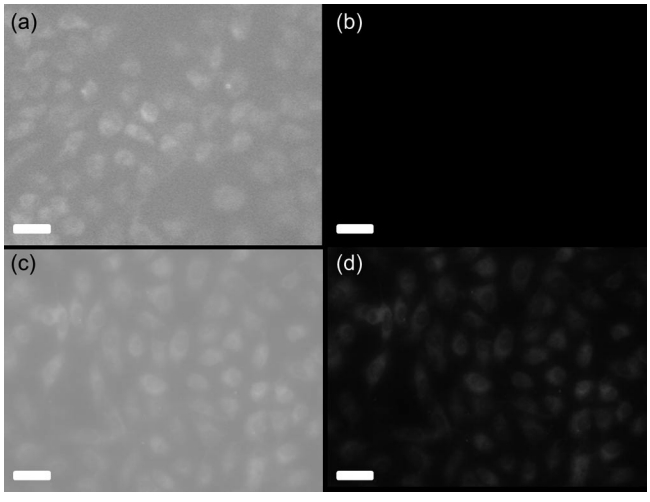

Figure 9. (a) Bright field image and (b) fluorescence microscopy image of SCABER cells loaded with **L1** (10 μM) incubated for 3 h. (c) Bright field image and (d) fluorescence microscope image of SCABER cells loaded with **L1** (10 μM) incubated for 3 h with the addition of Zn^{2+} (2 equiv.). Scale bar = 50 μM.

Conclusions

We have developed a fluorescent, colorimetric chemosensor based on 8-aminoquinoline for the detection of Zn^{2+} in living cells. **L1** displayed high selectivity, sensitivity, and a fast time response to Zn^{2+} in a physiological pH window with a 1:1 binding mode. The ability of **L1** to monitor intracellular Zn^{2+} in living cells was examined by fluorescence microscopy, which indicated that **L1** is cell-permeable and biocompatible. We hope that such Zn^{2+}-selective sensors will find application in biomedical and environmental detection.

Experimental Section

Materials and General Methods: ^1H and ^{13}C NMR spectra were recorded with a Varian Mercury-400 spectrometer with Me_4Si as the internal standard and $CDCl_3$ as the solvent. Mass spectra were performed with an HP-5988A spectrometer (EI at 70 eV). Absorption spectra were determined with a Varian UV-Cary 100 spectrophotometer. Fluorescence measurements were performed with a Hitachi F-4500 spectrofluorimeter. Both excitation and emission slits were 5 nm. Quantum yields were determined by an absolute method by using an integrating sphere with an Edinburgh Instrument FLS920. The pH values were adjusted by the addition of HCl (0.1 M) or NaOH (0.1 M). The volume of the added solutions was less than 20 μL to leave the concentration of **L1** unchanged. All pH measurements were carried with a pH-10C digital pH meter. All titration experiments were run twice for reliable data. All imaging experiments were performed with a fluorescence-inverted microscope (DMI 4000 B, Leica Microsystem) with excitation between 340 and 380 nm. The total magnification was 400×. The cationic solutions were prepared from $NaClO_4$, K_2CO_3, $Mg(ClO_4)_2$, $Ca(NO_3)_2$, $FeSO_4$, $Pb(NO_3)_2$,$Co(NO_3)_2$, $NiCl_2$, $Zn(NO_3)_2$, $Zn(ClO_4)_2$ $AgNO_3$, $CdSO_4$, $HgCl_2$, and $CuSO_4$ in distilled water with a concentration of 0.01 M or 0.001 M. The volume of the cationic solutions added was less than 100 μL to leave the concentration of **L1** unchanged. All synthetic materials were purchased from commercial suppliers and used without further purification. CH_3CN for spectroscopy was of HPLC reagent grade without fluorescent impurities.

Crystal Structure Determination: Single-crystal X-ray diffraction measurements were carried out with a Bruker SMART 1000 CCD diffractometer operating at 50 kV and 30 mA by using Mo-K_α radiation (λ = 0.71073 Å). The selected crystal was mounted inside a Lindemann glass capillary for data collection, which used the SMART and SAINT software.[16a,16b] An empirical absorption correction was applied by using the SADABS program.[16c] The structure was solved by direct methods and refined by full-matrix least squares on F^2 by using the SHELXTL-97 program package.[16d,16e] All non-hydrogen atoms were subjected to aniostropic refinement, and all hydrogen atoms were added in idealized positions and refined isotropically. Crystal data for **L1**: M_r = 640.77, triclinic, space group $P\bar{1}$, a = 10.4814(6) Å, b = 13.0286(7) Å, c = 13.1038(7) Å, α

= 79.464(3)°, β = 80.073(3)°, γ = 81.045(3), V = 1718.62(16) Å^3, Z = 2, $\rho_{calcd.}$ = 1.238 g cm^{-3}, R(reflections) = 0.0591(3051), wR_2(reflections) = 0.0974(6351). CCDC-825020 contains the supplementary crystallographic data for this paper. These data can be obtained free of charge from The Cambridge Crystallographic Data Centre via www.ccdc.cam.ac.uk/data_request/cif.

Preparation of 2-Chloro-*N*-(quinol-8-yl)acetamide: To a cooled, stirred solution of 8-aminoquinoline (288 mg, 2.0 mmol) and pyridine (0.23 mL, 2.8 mmol) was added a chloroform (10 mL) solution of 2-chloroacetyl chloride (0.15 mL, 2.0 mmol) dropwise over 1 h. After 2 h at room temperature, a brown-yellow solid was obtained by removing the solvent under reduced pressure. The crude product was purified by silica gel column chromatography using dichloromethane as eluent to afford 2-chloro-*N*-(quinol-8-yl)acetamide (362 mg, 80%).

Preparation of L1: 2-Chloro-*N*-(quinol-8-yl)acetamide (110 mg, 0.5 mmol), *N*-(rhodamine-6G)lactam-ethylenediamine (228 mg, 0.5 mmol), and potassium iodide (8 mg) were dissolved in acetonitrile (30 mL) with stirring and heated to reflux under nitrogen for 10 h. The mixture was cooled to room temperature, and the solvent was removed under reduced pressure to obtain a pale-yellow solid, which was purified by silica gel column chromatography using dichloromethane/petroleum ether (5:1, v/v) as eluent to afford **L1**. Yield: 83.8%. ^{1}H NMR (400 MHz): δ = 11.234 (s, 1 H), 8.743–8.738 (d, 1 H), 8.726–8.462 (m, 1 H), 8.101–8.076 (m, 1 H), 7.903–7.882 (m, 1 H), 7.505–7.424 (m, 4 H), 7.357–7.326 (m, 1 H), 7.075–7.055 (m, 1 H), 6.356 (s, 2 H), 6.253 (s, 2 H), 3.457 (s, 2 H), 3.402–3.372 (t, 2 H), 3.201 (s, 2 H), 3.126–3.110 (m, 4 H), 2.562–2.532 (t, 2 H), 1.805 (s, 6 H), 1.278–1.242 (t, 6 H) ppm. ^{13}C NMR (100 MHz): δ = 170.40, 168.69, 153.67, 148.39, 147.36, 138.84, 135.80. 134.33, 132.38, 131.13, 128.29, 127.93, 127.84, 127.03, 123.80, 122.75, 121.37, 121.28, 117.90, 116.20, 105.82, 96.42, 65.14, 53.19, 48.23, 40.03, 38.18, 16.41, 14.57 ppm. ESI-MS: 641.1 $[M + 1]^+$.

Cell Incubation and Imaging: The SCABER cells were provided by Cells Bank of the Chinese Academy of Science (Shanghai, China). Cells were grown in H-DMEM (high glucose) supplemented with 10% FBS in an atmosphere of 5% CO_2/95% air at 37 °C. Cells (5×10^8/L) were plated on 18 mm glass coverslips and allowed to adhere for 24 h. Uptake experiments of Zn^{2+} were performed in the same medium supplemented with 20 μM $Zn(NO_3)_2$ for 0.5 h. Before the experiments, cells were washed with phosphate-buffered saline (PBS) and incubated with 10 μM **L1** at 37 °C for 3 h. Cell imaging was carried out after washing the cells with PBS.

Assessment of Biocompatibility: The biocompatibility was determined in L929 mouse fibroblast cell lines. The cell viability was evaluated by using the modified MTT assay. The cells were plated at a density of 1×10^5 in 96-well plates 24 h prior to exposure to the materials. Different concentrations of **L1** with saturated surfaces [by interaction with DMEM/F12 (1:1) for 24 h before use] were added to the wells, and the cells were incubated for 24, 48, and 72 h. After treatment, 10 μL of MTT (5 mg mL^{-1} in PBS) was added into each well. After 4 h of incubation, culture supernatants were aspirated, and purple insoluble MTT product was redissolved in dimethyl sulfoxide (150 μL) over 10 min. The concentration of the reduced MTT in each well was determined spectrophotometrically by subtraction of the absorbance reading at 630 nm from that measured at 570 nm using a microplate reader. All MTT experiments were performed five times, and the maximum and minimum were discounted. The results were expressed as the mean ± standard deviation. Cell viabilities were presented as the percentage of the absorbance of **L1**-treated cells to the absorbance of control cells.

Supporting Information (see footnote on the first page of this article): Materials and general methods; schematic molecular structures; experimental details; additional NMR and ESI-MS data.

Acknowledgments

This study was supported by the Fundamental Research Funds for the Central University (Lzujbky-2011-18), the Foundation of Key Laboratory of Nonferrous Metals Chemistry and Resources Utilization of Gansu Province, and the State Key Laboratory of Applied Organic Chemistry.

[1] a) A. P. De Silva, H. Q. N. Gunaratne, T. Gunnlaugsson, A. J. M. Huxley, C. P. McCoy, J. T. Rademacher, T. E. Rice, *Chem. Rev.* **1997**, *97*, 1515; b) L. Prodi, F. Bolletta, M. Montalti, N. Zaccheroni, *Coord. Chem. Rev.* **2000**, *205*, 59; c) J. S. Kim, D. T. Quang, *Chem. Rev.* **2007**, *107*, 3780; d) H. N. Kim, M. H. Lee, H. J. Kim, J. S. Kim, J. Yoon, *Chem. Soc. Rev.* **2008**, *37*, 1465.

[2] a) B. Valeur, I. Leray, *Coord. Chem. Rev.* **2000**, *205*, 3; b) K. Rurack, U. Resch-Genger, *Chem. Soc. Rev.* **2002**, *31*, 116; c) V. Amendola, L. Fabbrizzi, F. Forti, M. Licchelli, C. Mangano, P. Pallavicini, A. Poggi, D. Sacchi, A. Taglieti, *Coord. Chem. Rev.* **2006**, *250*, 273.

[3] a) A. W. Czarnik, *Fluorescent Chemosensors for Ion and Molecule Recognition*, American Chemical Society, Washington, DC, **1993**; b) A. P. de Silva, D. B. Fox, A. J. M. Huxley, T. S. Moody, *Coord. Chem. Rev.* **2000**, *205*, 41; c) Q. W. He, E. W. Miller, A. P. Wong, C. J. Chang, *J. Am. Chem. Soc.* **2006**, *128*, 9316.

[4] a) T. V. O'Halloran, *Science* **1993**, *261*, 715; b) J. Y. Koh, S. W. Suh, B. J. Gwag, Y. Y. He, C. Y. Hsu, D. W. Choi, *Science* **1996**, *272*, 1013; c) F. Walker, R. E. Black, *Annu. Rev. Nutr.* **2004**, *24*, 255; d) C. J. Frederickson, A. I. Bush, *Biometals* **2001**, *14*, 353.

[5] a) K. Kiyose, H. Kojima, Y. Urano, T. Nagano, *J. Am. Chem. Soc.* **2006**, *128*, 6548; b) K. Komatsu, Y. Urano, H. Kojima, T. Nagano, *J. Am. Chem. Soc.* **2007**, *129*, 13447; c) C. R. Goldsmith, S. J. Lippard, *Inorg. Chem.* **2006**, *45*, 555; d) B. A. Wong, S. Friedle, S. J. Lippard, *J. Am. Chem. Soc.* **2009**, *131*, 7142; e) A. E. Dennis, R. C. Smith, *Chem. Commun.* **2007**, 4641; f) J. F. Zhu, H. Yuan, W. H. Chan, A. W. M. Lee, *Org. Biomol. Chem.* **2010**, *8*, 3957; g) Z. C. Xu, J. Y. Yoon, D. R. Spring, *Chem. Soc. Rev.* **2010**, *39*, 1996; h) Z. C. Xu, K. H. Baek, H. N. Kim, J. N. Cui, X. H. Qian, D. R. Spring, I. Shin, J. Yoon, *J. Am. Chem. Soc.* **2010**, *132*, 601; i) Z. C. Xu, G. H. Kim, S. J. Han, M. J. Jou, C. Lee, I. Shin, J. Yoon, *Tetrahedron* **2009**, *65*, 2307.

[6] K. Rurack, *Spectrochim. Acta, Part A* **2001**, *57*, 2161.

[7] P. Jiang, Z. J. Guo, *Coord. Chem. Rev.* **2004**, *248*, 205.

[8] a) I. B. Mahadevan, M. C. Kimber, S. F. Lincoln, E. R. Tiekink, A. D. Ward, W. H. Betts, I. J. Forbes, P. D. Zalewski, *Aust. J. Chem.* **1996**, *49*, 561; b) P. D. Zalewski, I. J. Forbes, W. H. Betts, *Biochem. J.* **1993**, *296*, 403; c) C. J. Frederickson, E. J. Kasarskis, D. Ringo, R. E. Frederickson, *J. Neurosci. Methods* **1987**, *20*, 91; d) C. J. Frederickson, *J. Int. Rev. Neurobiol.* **1989**, *31*, 145.

[9] Y. Liu, N. Zhang, Y. Chen, L. H. Wang, *Org. Lett.* **2007**, *9*, 315.

[10] a) H. A. Benesi, J. H. Hildebrand, *J. Am. Chem. Soc.* **1949**, *71*, 2703; b) M. Barra, C. Bohne, J. C. Scaiano, *J. Am. Chem. Soc.* **1990**, *112*, 8075.

[11] a) K. Hiratani, T. J. Hirose, K. Kasuga, K. Saito, *J. Org. Chem.* **1992**, *57*, 7083; b) T. Yang, C. Tu, J. Y. Zhang, L. P. Lin, X. M. Zhang, Q. Liu, J. Ding, Q. Xu, Z. J. Guo, *Dalton Trans.* **2003**, 3419.

[12] P. J. Jiang, L. Z. Chen, J. Lin, Q. Liu, J. Ding, X. Gao, Z. J. Guo, *Chem. Commun.* **2002**, 1424.

[13] a) L. Huang, X. Wang, G. Q. Xie, P. X. Xi, Z. P. Li, M. Xu, Y. J. Wu, D. C. Bai, Z. Zeng, *Dalton Trans.* **2010**, *39*, 7894; b) P. X. Xi, L. Huang, H. Liu, P. F. Jia, F. J. Chen, M. Xu, Z. Z. Zeng, *J. Biol. Inorg. Chem.* **2009**, *14*, 815; c) P. X. Xi, L. Huang, G. Q. Xie, F. J. Chen, Z. H. Xu, D. C. Bai, Z. Z. Zeng, *Dalton Trans.* **2011**, *40*, 6382–6384.
[14] K. M. Hendrickson, T. Rodopoulos, P. A. Pittet, I. Mahadevan, S. F. Lincoln, A. D. Ward, T. Kurucsev, P. A. Duckworth, I. J. Forbes, P. D. Zalewski, W. H. Betts, *J. Chem. Soc., Dalton Trans.* **1997**, 3879.
[15] Y. Chen, K. Y. Han, Y. Liu, *Bioorg. Med. Chem.* **2007**, *15*, 4537.
[16] a) Bruker, *SMART*, version 5.622, Bruker AXS Inc., Madison, Wisconsin, USA, **1997**; b) Bruker, *SAINT*, version 6.02, Bruker AXS Inc., Madison, Wisconsin, USA, **1999**; c) G. M. Sheldrick, *SADABS*, version 2.03, University of Göttingen, Germany, **1996**; d) G. M. Sheldrick, *SHELXL-97*, *Program for the Solution of Crystal Structures*, University of Göttingen, Göttingen, Germany, **1997**; e) G. M. Sheldrick, *SHELXL-97*, *Program for the Refinement of Crystal Structures*, University of Göttingen, Göttingen, Germany, **1997**.

Received: August 1, 2011
Published Online: December 8, 2011

